Geol. Bull. Univ. Peshawar, 1986, Vol. 19, pp. 157–182

PRELIMINARY PETROCHEMICAL STUDY OF THE CHILAS COMPLEX, KOHISTAN ISLAND ARC, NORTHERN PAKISTAN

S. HAMIDULLAH and M.Q. JAN
National Centre of Excellence in Geology, University of Peshawar

ABSTRACT

The Chiles complex, streaching more than 300 km and reaching 40 km in width, consists predominantly of gabbronorites with minor pyroxenites, anorthosites and quartz diorites containing labradorite/andesine. Within these are found upto 4 km², seemingly intrusive, masses of dunite-perodite-troctolite-anorthosite association characterised by the presence of bytownite/anorthite. Sixty four new chemical analyses reflect a genetic relationship among the various rock types. The data suggest crystallization from an arc-related parent magma of calcalkaline character. The oxides vs. D.I. and CMAS plots indicate olivine, orthopyroxene, and plagioclase as the dominant liquidus phases for the development of rocks varying from ultramafic through mafic to intermediate compositions. It is concluded that crystallization occurred possibly at a depth of <25 km followed by pyroxene granulite facies metamorphism. This was followed by widspread amphibolitisation during uplift. The masses of ultramafic and related rocks appear to be early cummulates that were remobilized and emplaced into the main gabbronorite association.

INTRODUCTION

The Chilas complex represents lower level rocks of the Late Jurassic-Cretaceous Kohistan island arc. It extends for 300 km from Nanga Parbat through Swat to south-central Dir and attains a width of 40 km in the middle (Fig. 1). The field relationship, petrography and chemistry of the different parts of this extensive horizon have been described by several workers (Jan and Mian, 1971; Jan and Kampe, 1971; Chowdhry *et al.*, 1974, Shams, 1975; Jan, 1977a; 1980; Jan and Howie 1980; Jan *et al.*, 1984; Asif *et al.*, 1985). Majority of the rocks correspond to feldspathic gabbronorite composition and consist of plagio-

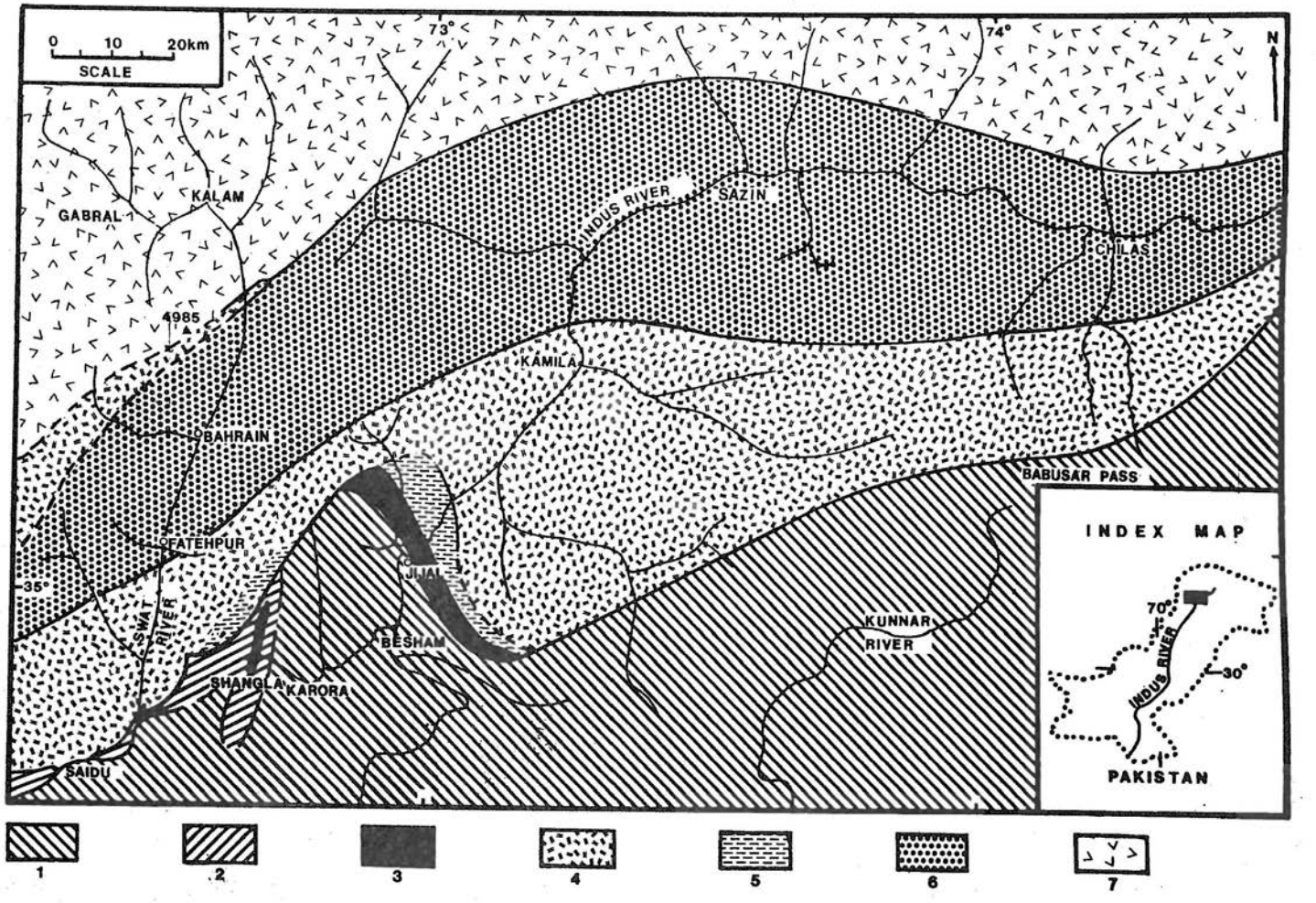

Fig. 1. Geological map of the south-central Kohistan zone, northern Pakistan (after Jan 1979)———; 1. Palaeozoic to Precambrian metasediments and younger granites, 2. Shangla-Kabal high-pressure metamorphic zone with blue-schist, 3. Alpine ultramafic rocks, 4. Southern amphibolite belt, 5. High-pressure Jijal garnet granulite, 6. Pyroxene granulite-retrograde amphibolite belt, 7. Intermediate to silicic plutonics, calcalkaline volcanics, amphibolites and metasediments.

clase (An_{45-61}), ortho– and clinopyroxene with small amounts of quartz, opaque minerals (magnetite, titanmagnetite, ilmenite), hornblende, biotite, and apatite. The intermediate members contain a relatively higher proportion of quartz and may also contain some K-feldspar. Scapolite occurs in a few rocks but garnet is restricted to secondary veins, The rocks display features typical of layered complexes, i.e. rhythmic layering and graded and current bedding. While many of the layers are noritic, some are pyroxenitic, anorthositic, peridotitic and troctolitic (see Jan, 1980, p. 102). The rocks were considered to be of igneous origin by earlier workers, on the basis of petrographic and mineralogic characters, Jan (1977a) and Jan and Howie (1980) considered these to be of meta-igneous origin having been uniformally crystallized under pyroxene-granulite facies environments at about 800°C under 5.5–7 kb pressure.

Small to large masses of amphibolites (metamorphosed gabbronorite and related rocks) occur intimately associated with pyroxene granulite (gabbronorite) and make over a forth of the belt. On the basis of similar chemistry, Jan (1980) considered the two types of the rocks to be cogenetic and pointed two possibilities for the production of the two different types; (a) either both represent recrystallised norites at similar temperature and pressure at the same time and the availability of water having played a role in producing hornblende instend of pyroxene or (b) the amphibalites, especially abundant along the southern margin of the granulite belt, are retrograde products of the granulites, mainly due to influx of water during the obduction of the latter. The gabbronorite and amphibolites together with related rocks have been classified as the main noritic association by Jan *et al.*, (1984) and Asif *et al.*, (1985).

Apart from amphibolites, large bodies of ultramafic rocks including dunite, peridotite, chromitite, pyroxenites, troctolite, norite, anorthosite and pyroxene-olivine pagmatites, seemingly intrusive in gabbronorite and recrystallized in granulite facies occur in the Chilas complex. Such rocks as a whole have been classified as ultramafic association by Asif *et al.*, (1985; see also Jan *et al.*, 1984). Olivine is an important constituent of the ultramatic rocks and troctolites which are characteristically devoid of quartz, biotite and apatite. The pyroxenes and plagioclase (An_{95-69}) of these rocks are more basic as compared to those in rocks of the main noritic association, whereas the dominant opaque minerals are chrom spinel and some sulphides. Sedimentary structures, particularly layring is more common than in rocks of the main noritic association.

The aim of the present study is to present some new chemical data (see Table 1) describe affinites and igneous crystallization histories of the various rock types and investigate their genetic relationship. Sixty four samples from the various rock types of the two associations (new data; for details see Table 1; Fig. 2) in conjunction with one corona gabbro and four norite analyses (Shams, 1975) have been used for plotting on various diagrams.

TABLE 1. SHOWING CHEMICAL DATA OF ROCKS FROM THE CHILAS COMPLEX

S. No.	1	2	3	4	5	6	7
Sample	IK505	IK507	IK417	SK326B	US26	SK586	US24
SiO_2	37.56	37.68	42.42	45.05	48.00	48.46	50.80
TiO_2	0.00	0.19	0.10	0.24	0.21	0.58	0.69
Al_2O_3	0.54	1.05	2.66	4.00	14.15	6.57	5.30
Fe_2O_3	5.06	4.59	3.76	4.24	1.41	3.69	2.27
FeO	7.73	8.23	8.20	15.37	5.50	6.60	6.54
MnO	0.22	0.22	0.18	0.34	0.13	0.22	0.20
MgO	47.98	47.03	35.54	25.45	16.85	24.86	18.15
CaO	0.32	0.42	5.70	4.17	12.58	6.18	14.50
Na_2O	0.23	0.08	0.20	0.27	0.84	0.30	0.46
K_2O	0.04	0.04	0.03	0.05	0.06	0.10	0.19
P_2O_5	0.00	0.00	0.00	0.03	0.11	0.12	0.09
H_2O+	0.00	0.00	0.00	0.31	1.29	2.28	0.93
Total	99.68	99.53	98.79	99.52	101.13	99.96	100.12
Rb	—	—	—	<10	10	16	10
Ba	—	—	—	—	—	<30	—
Sr	—	—	—	90	103	15	63
Cr	—	—	—	1276	1117	1725	3440
Ni	—	—	—	546	522	793	280
Zr	—	—	—	<10	<10	12	≤10
Cu	—	—	—	<30	74	44	33
Y	—	—	—	<10	14	<10	20
Co	—	—	—	314	50	75	55
Ga	—	—	—	10	<10	<10	≤10
Zn	—	—	—	93	<30	83	59
			C. I. P. W. NORMS				
or	0	0	0	0	0	1	1
ab	0	0	2	2	7	3	4
an	0	2	6	10	35	16	12
ne	1	0	0	0	0	0	0
di	0	0	17	9	21	11	47
hy	0	0	7	39	16	50	26
ol	89	88	61	32	18	11	5
mt	7	7	5	6	2	5	3
il	0	0	0	0	0	1	1
wus	2	2	0	0	0	0	0

Table 1 continued

S. No.	8	9	10	11	12	13	14
Sample	SK340	SK315	IK415	SI246	IK422	IK980	SK535
SiO_2	52.15	52.90	45.05	50.89	43.25	48.39	53.79
TiO_2	0.32	0.43	0.26	0.32	0.05	0.09	0.83
Al_2O_3	5.75	7.37	8.05	3.70	14.13	21.28	18.05
Fe_2O_3	1.40	1.20	5.36	1.41	7.28	1.62	3.33
FeO	10.11	10.51	6.80	6.17	1.47	2.61	5.40
MnO	0.23	0.30	0.22	0.08	0.12	0.07	0.21
MgO	25.40	17.19	25.45	21.00	23.32	8.83	5.60
CaO	3.68	8.75	3.83	16.56	8.44	12.31	9.13
Na_2O	0.23	0.57	1.80	0.27	1.12	1.98	3.82
K_2O	0.03	0.13	0.19	0.03	0.02	0.08	0.38
P_2O_5	0.00	0.11	0.00	0.11	0.00	0.00	0.14
H_2O+	0.51	0.78	0.00	0.67	0.00	0.00	1.28
H_2O-	0.14	0.00	0.00	0.00	0.00	0.00	0.00
Total	99.95	100.24	97.01	101.21	99.20	97.26	101.96
Rb	<10	10	—	<10	—	—	45
Ba	—	—	—	—	—	—	120
Sr	75	93	—	20	—	—	429
Cr	42	30	—	1148	—	—	84
Ni	503	273	—	397	—	—	125
Zr	<10	33	—	<10	—	—	46
Cu	10	35	—	252	—	—	41
Y	<10	22	—	<10	—	—	<10
Co	14	112	—	54	—	—	35
Ga	10	35	—	<10	—	—	<10
Zn	<30	127	—	<30	—	—	123
			C. I. P. W. NORMS				
Q	0	2	0	0	0	0	3
or	0	1	1	0	0	0	2
ab	2	5	15	2	9	17	32
an	15	17	13	9	33	49	31
di	3	21	4	58	7	10	11
hy	72	51	19	14	7	14	15
ol	5	0	36	15	34	5	0
mt	2	2	8	2	5	2	5
il	1	1	0	1	0	0	2
hem	0	0	0	0	4	0	0

Table 1 continued

S. No.	15	16	17	18	19	20	21
Sample	188A	SI188B	SI182	SI217	SI190	SI197	A
SiO_2	49.81	49.53	50.40	49.88	50.20	51.56	51.61
TiO_2	1.08	1.20	0.88	1.48	1.46	0.87	0.47
Al_2O_3	18.43	18.78	18.88	18.75	19.20	18.40	17.13
Fe_2O_3	3.58	4.33	2.13	2.42	3.27	2.26	1.75
FeO	7.29	6.87	7.25	7.48	6.79	6.21	7.41
MnO	0.19	0.19	0.20	0.14	0.23	0.16	0.18
MgO	5.65	4.81	5.98	6.42	5.70	5.42	7.95
CaO	10.08	9.66	10.28	9.45	11.15	9.62	9.88
Na_2O	2.95	3.27	2.98	3.22	3.16	3.25	2.69
K_2O	0.27	0.33	0.21	0.51	0.22	0.42	0.29
P_2O_5	0.27	0.35	0.22	0.29	0.14	0.22	0.02
H_2O+	0.16	0.15	0.13	0.58	0.57	0.44	0.48
H_2O-	0.11	0.42	0.05	0.00	0.00	0.30	0.03
Total	99.87	99.89	99.57	100.62	102.09	99.13	99.89
Rb	<10	12	<10	<10	14	<10	20
Ba	180	135	<30	<30	<30	<30	75
Sr	362	395	351	351	491	360	>1000
Cr	89	88	65	39	104	135	350
Ni	25	25	108	48	15	40	150
Zr	33	61	51	81	35	54	50
Cu	194	75	33	73	67	57	95
Y	<10	10	19	19	15	15	<10
Co	37	42	48	48	44	44	—
Ga	<10	26	10	<10	35	35	—
Zn	60	52	90	90	33	33	140
			C. I. P. W. NORMS				
Q	1	1	0	0	0	2	0
or	2	2	1	3	1	2	2
ab	25	28	25	27	27	28	23
an	36	36	37	35	38	34	34
di	10	8	10	8	14	10	12
hy	18	15	20	14	12	17	25
ol	0	0	1	5	2	0	1
mt	5	6	3	4	5	3	3
il	2	2	2	3	3	2	1
ap	1	1	1	1	0	1	0

Table 1 continued

S. No. Sample	22 SK367	23 SK322	24 SK470	25 SI337	26 SI341	27 SI196	28 US15
SiO_2	52.02	52.24	52.99	52.26	53.05	53.11	53.30
TiO_2	0.54	0.86	0.93	0.93	0.63	1.49	1.42
Al_2O_3	19.75	14.34	19.74	17.47	19.05	19.15	17.47
Fe_2O_3	1.88	1.73	1.23	1.83	1.12	1.68	3.10
FeO	5.48	8.16	6.41	8.57	8.08	7.37	6.21
MnO	0.18	0.31	0.22	0.22	0.18	0.17	0.17
MgO	5.58	10.70	5.61	6.15	5.56	5.57	4.65
CaO	9.80	9.62	9.53	10.41	10.03	9.20	8.60
Na_2O	3.50	2.75	3.41	2.37	2.64	3.37	3.23
K_2O	0.35	0.23	0.46	0.51	0.45	0.38	1.10
P_2O_5	0.13	0.07	0.23	0.11	0.12	0.19	0.50
H_2O+	0.64	0.86	0.32	0.53	0.46	0.27	0.36
H_2O-	0.00	0.00	0 00	0.00	0.00	0.00	0.19
Total	99.85	101.87	101.08	101.36	101.37	101.95	100.30
Rb	13	<10	35	<10	13	<10	29
Ba	<30	<30	54	140	120	180	260
Sr	409	262	404	333	217	306	350
Cr	72	82	130	130	111	<15	76
Ni	15	65	41	60	15	60	50
Zr	47	40	40	47	35	70	145
Cu	41	69	39	51	44	77	235
Y	<10	<10	<10	24	16	<10	34
Co	25	65	31	40	30	26	28
Ga	<10	12	18	<10	22	29	<10
Zn	78	115	65	90	72	30	30
			C. I. P. W. NORMS				
Q	0	0	1	3	3	2	5
or	2	1	3	3	3	2	7
ab	30	23	29	20	22	29	27
an	37	26	37	36	39	36	30
di	9	17	7	13	8	7	8
hy	18	23	20	22	23	21	15
ol	0	6	0	0	0	0	0
mt	3	3	2	3	2	2	4
il	1	2	2	2	1	3	3
ap	0	0	1	0	0	0	1

Table 1 continued

S. No.	29	30	31	32	33	34	35
Sample	SK338	US9	B	SK600	SI192	SK528	SK521
SiO_2	53.31	53.36	53.36	53.37	53.40	53.62	54.00
TiO_2	0.82	0.42	0.74	0.52	0.45	0.88	0.94
Al_2O_3	18.82	18.61	17.72	19.45	18.81	17.63	17.75
Fe_2O_3	1.95	1.70	1.33	1.73	1.70	2.07	1.76
FeO	5.91	5.70	6.59	5.20	5.56	5.94	6.91
MnO	0.16	0.16	0.16	0.14	0.14	0.14	0.18
MgO	5.88	6.02	6.60	5.39	6.31	5.55	5.46
CaO	9.03	9.73	8.87	9.69	9.38	8.80	9.30
Na_2O	3.45	3.08	3.30	3.42	2.94	3.14	3.50
K_2O	0.69	0.53	0.62	0.42	0.49	0.77	0.69
P_2O_5	0.17	0.18	0.12	0.04	0.06	0.15	0.19
H_2O+	1.50	0.59	0.34	0.38	0.24	0.80	0.38
H_2O-	0.00	0.15	0.06	0.10	0.15	0.05	0.00
Total	101.69	100.23	99.81	99.85	99.63	99.54	101.06
Rb	10	<10	20	14	12	11	31
Ba	202	55	150	35	217	277	185
Sr	366	362	1000	399	360	313	356
Cr	25	100	175	92	56	82	64
Ni	26	30	100	20	90	50	26
Zr	93	53	100	15	71	90	100
Cu	259	37	200	48	60	181	165
Y	11	19	—	11	11	<10	11
Co	35	27	—	17	17	30	30
Ga	19	44	—	19	<10	<10	<10
Zn	44	63	112	76	104	78	117
			C. I. P. W. NORMS				
Q	1	3	1	2	3	4	2
or	4	3	4	2	3	5	4
ab	29	26	28	29	25	27	30
an	34	35	32	36	37	32	31
di	8	10	9	9	8	9	12
hy	19	19	22	16	20	18	18
mt	3	2	2	3	2	3	3
il	2	1	1	1	1	2	2

Table 1 continued

S. No.	36	37	38	39	40	41	42
Sample	SK508	SK301	DTD	S1221	SK615	SK422	S1153
SiO_2	54.24	54.50	54.95	55.07	56.13	56.46	56.82
TiO_2	1.06	0.57	0.91	1.34	0.67	0.66	1.32
Al_2O_3	17.86	19.32	17.17	16.95	18.93	18.76	15.76
Fe_2O_3	2.28	2.28	2.22	2.35	1.97	3.15	3.00
FeO	6.01	5.15	5.65	7.14	5.29	4.00	6.09
MnO	0.17	0.12	0.16	0.20	0.14	0.14	0.17
MgO	5.51	5.90	6.61	5.68	4.00	4.02	3.82
CaO	8.28	8.70	8.82	7.80	7.91	7.93	7.71
Na_2O	3.37	3.68	3.13	3.57	3.56	3.61	3.17
K_2O	0.87	0.67	0.56	0.57	0.74	0.59	0.63
P_2O_5	0.28	0.12	0.23	0.34	0.20	0.19	0.36
H_2O+	0.35	0.84	0.53	0.47	0.11	0.23	0.14
H_2O-	0.00	0.00	0.00	0.00	0.06	0.11	0.56
Total	100.28	101.85	100.93	101.48	99.71	99.85	99.55
Rb	20	35	16	14	14	<10	10
Ba	75	140	<30	50	61	50	235
Sr	325	368	380	331	524	470	297
Cr	109	60	135	147	<15	<15	60
Ni	94	43	108	53	100	25	74
Zr	78	50	31	90	55	65	165
Cu	46	52	70	77	40	40	68
Y	21	<10	23	11	14	—	21
Co	30	35	23	53	27	18	24
Ga	14	<10	21	<10	<10	<10	10
Zn	76	43	60	103	118	135	135
			C. I. P. W. NORMS				
Q	4	2	6	5	8	10	14
or	5	4	3	3	4	3	4
ab	29	31	26	30	30	31	27
an	31	34	31	29	33	33	27
di	7	7	9	6	4	4	7
hy	18	18	19	20	15	12	13
mt	3	3	3	3	3	5	4
il	2	1	2	3	1	1	3
ap	1	0	1	1	0	0	1

Table 1 continued

S. No.	43	44	45	46	47	48	49
Sample	SK592	SK512	US14	C	IK867	A	SK395
SiO_2	56.85	56.95	58.23	59.17	47.58	47.44	49.01
TiO_2	0.79	0.95	1.05	0.93	0.17	0.91	0.84
Al_2O_3	18.30	17.21	16.73	16.41	22.11	17.92	19.30
Fe_2O_3	1.30	2.70	2.71	1.80	2.97	2.25	1.49
FeO	5.15	5.49	4.64	5.04	3.76	7.62	6.24
MnO	0.11	0.16	0.12	0.13	0.10	0.19	0.14
MgO	4.15	5.87	3.79	3.72	9.13	8.12	6.94
CaO	7.91	7.30	6.95	6.16	12.35	10.38	12.32
Na_2O	3.46	3.80	3.74	3.84	1.95	1.78	2.87
K_2O	0.67	0.72	1.73	1.58	0.05	0.34	0.32
P_2O_5	0.15	0.27	0.27	0.24	0.00	0.26	0.15
H_2O+	1.04	0.63	0.17	0.42	0.00	1.60	1.59
H_2O-	0.04	0.00	0.07	0.05	0.00	0.10	0.00
Total	99.92	102.05	100.20	99.49	100.17	99.91	101.21
Rb	14	<10	34	22	—	24	11
Ba	108	100	50	50	—	50	155
Sr	368	356	34	1000	—	1000	408
Cr	45	30	60	75	—	150	132
Ni	74	26	50	30	—	100	173
Zr	72	190	230	200	—	152	23
Cu	30	310	150	150	—	295	<30
Y	11	22	30	50	—	10	<10
Co	21	25	20	—	—	—	37
Ga	<10	13	45	—	—	—	10
Zn	103	30	119	136	—	140	21
			C. I. P. W.	NORMS			
Q	9	7	10	11	0	0	0
or	4	4	10	9	0	2	2
ab	29	32	32	32	17	24	24
an	32	28	24	23	51	35	39
di	5	5	7	5	8	12	17
hy	15	19	11	13	10	5	1
ol	0	0	0	0	10	15	13
mt	2	4	4	3	4	3	2
il	2	2	2	2	0	2	2
ap	0	1	1	1	0	1	0

Table 1 continued

S. No.	50	51	52	53	54	55	56
Sample	US8	SK504	SK301B	SK531	SK477	S1188C	S1281
SiO_2	49.07	50.20	51.62	51.91	52.41	52.42	52.50
TiO_2	0.64	0.98	1.60	0.70	0.59	0.88	0.72
Al_2O_3	19.98	18.57	18.17	17.78	18.23	18.03	18.14
Fe_2O_3	2.84	4.68	2.89	3.98	3.33	3.54	3.18
FeO	5.44	5.84	5.20	5.31	5.78	4.78	5.35
MnO	5.15	0.22	0.19	0.19	0.18	0.14	0.19
MgO	5.55	5.80	6.64	5.96	6.95	4.46	5.04
CaO	10.34	10.05	8.28	8.67	9.12	9.11	9.43
Na_2O	3.69	3.32	3.14	3.60	3.40	3.46	3.70
K_2O	0.47	0.41	0.70	0.78	0.28	0.89	0.50
P_2O_5	0.25	0.25	0.11	0.12	0.15	0.14	0.28
H_2O+	1.65	1.42	2.07	1.70	1.19	1.55	2.55
H_2O-	0.08	0.00	0.00	0.00	0.00	0.06	0.00
Total	100.15	101.62	100.61	100.70	101.61	99.46	101.58
Rb	35	10	38	41	<10	10	35
Ba	69	121	375	375	30	122	43
Sr	486	347	439	281	316	366	325
Cr	115	150	112	149	82	25	76
Ni	61	110	60	43	68	28	50
Zr	93	47	55	70	40	60	52
Cu	600	230	60	115	30	82	43
Y	11	20	28	<10	31	12	18
Co	38	45	38	36	43	42	46
Go	32	15	29	16	34	30	<10
Zn	35	78	61	56	98	100	22
			C. I. P. W. NORMS				
Q	0	0	3	1	1	4	2
or	3	2	4	5	2	5	3
ab	31	28	27	30	29	29	31
an	37	35	33	30	34	31	31
di	11	11	6	10	9	11	11
hy	0	15	19	16	20	11	14
ol	11	0	0	0	0	0	0
mt	4	7	4	6	5	5	5
il	1	2	3	1	1	2	1
ap	1	1	0	0	0	0	1

Table 1 continued

S. No.	57	58	59	60	61	62	63
Sample	SK407	SK538A	SI194	IK854	SI185	KDM	SK506
SiO_2	52.59	53.55	54.50	45.42	46.41	53.09	53.33
TiO_2	0.46	0.77	0.87	0.68	0.13	0.24	0.43
Al_2O_3	19.59	18.72	17.75	22.43	28.95	27.13	26.78
Fe_2O_3	2.29	2.66	1.71	5.64	0.83	0.50	0.87
FeO	5.59	5.08	5.77	3.67	0.60	1.55	1.56
MnO	0.16	0.17	0.15	0.07	0.03	0.04	0.04
MgO	5.90	5.50	4.75	6.49	0.90	2.17	2.20
CaO	0.12	0.25	8.90	11.91	15.60	10.69	8.70
Na_2O	3.83	3.30	3.32	1.88	3.05	4.41	4.75
K_2O	5.50	0.80	0.56	0.08	1.02	0.54	1.06
P_2O_5	0.12	0.11	0.19	0.00	0.00	0.13	0.13
H_2O+	1.73	1.88	1.84	0.00	1.89	0.17	0.83
H_2O-	0.00	0.00	0.00	0.00	0.06	0.00	0.00
Total	101.88	101.79	100.31	98.27	99.47	100.66	100.68
Rb	<10	17	44	—	20	10	11
Ba	115	120	220	—	255	80	112
Sr	390	348	329	—	1260	803	570
Cr	173	179	<15	—	<15	15	55
Ni	110	71	80	—	<15	26	35
Zr	32	70	110	—	<10	<10	50
Cu	105	80	68	—	50	151	88
Y	<10	17	20	—	<10	23	13
Co	35	35	33	—	<10	<10	<10
Ga	<10	13	<10	—	18	<10	57
Zn	112	60	67	—	30	<30	<30
			C. I. P. W.	NORMS			
Q	0	3	6	0	0	0	0
or	3	5	3	0	6	3	6
ab	32	28	28	16	11	37	40
an	35	34	32	53	62	52	42
ne	0	0	0	0	8	0	0
C	0	0	0	0	0	0	2
di	8	9	9	5	5	0	0
hy	15	15	15	15	0	3	5
wo	0	0	0	0	3	0	0
ol	3	0	0	0	0	4	2
mt	3	4	2	8	1	1	1
il	1	1	2	1	0	0	1

Explanation of Table 1

1–2 = Dunite; 3–7 = Peridotite; 8–10 = Orthopyroxenite; 11 = Clinopyroxenite; 12 = Troctolite; 13 = Olivine gabbro; 14–47 = Gabbronorite; 48–59 = Amphibolite; 60 = Pyroxene pegmatite; 61–63 = Anorthosite.

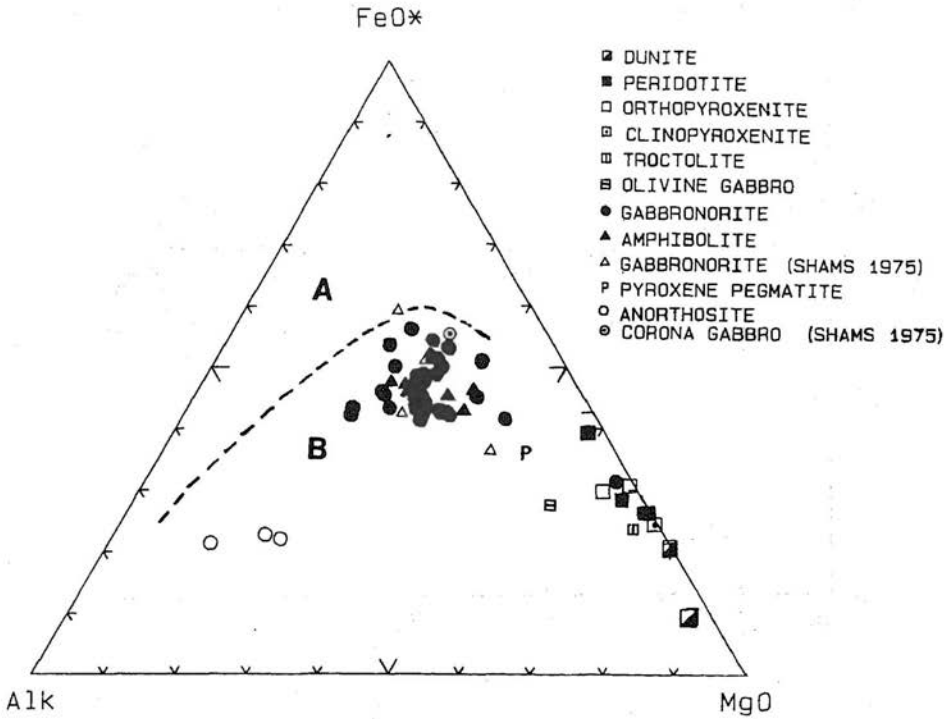

Fig. 2. AFM plot of the Chilas complex rocks. A = Tholeiitic, B = Calcalkaline; Irvine & Barager (1971).

AFFINITY DESCRIPTION

Excluding the cummulate rocks (ultramafic rocks and anorthosites) majority of the rest of compositions plot in the field of calcalkaline rocks on AFM plot and Al_2O_3 *vs* An plot of Irvine and Bargar (1971), whereas on FeO–MgO–Al_2O_3 plot such rocks occupy the field of orogenic environments (Fig. 2–4). On a TiO_2–MnO–P_2O_5 plot of Mullan (1983) and Ti–Zr–Sr plot of Pearce *et al.*, (1977) these rocks show a scatter and mostly plot in the field of arc lavas and none falls in the field of ocean floor basalts (plots not presented). All these features indicate that the parent magma for the Chilas complex was calcalkaline produced in orogenic environments of island arc type, a feature supported by the mineral chemistry also (Jan, 1986).

OXIDE *VS* DIFFERENTIATION INDEX (D.I.) PLOTS

The continuous variation in major element chemistry is well represented by oxide *vs* D.I. plots. The regular trends shown on Na_2O, SiO_2, Al_2O_3, CaO, MgO, FeO, MnO and K_2O *vs* D.I. plots of the majority of the basic-intermediate rocks (D.I. > 15) reflect fractionation and the progressive development of basic

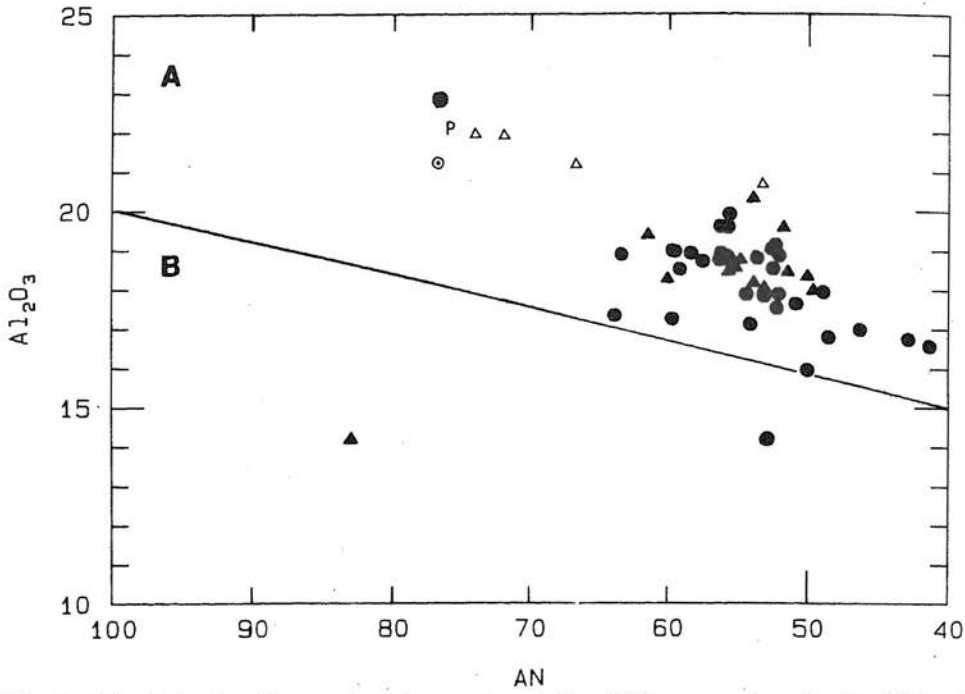

Fig. 3. Discrimination diagram showing rocks of the Chilas complex in the field of calcalkaline rocks. A = Calcalkaline, B = Tholeiitic; Irvine & Barager (1971); Symbols as in Fig. 2.

to intermediate rock types (Figs. 5a–f, i, j). Plots of the ultramafic rocks (D.I. < 10) represent a continuation of the trend of the basic-intermediate types on Na_2O *vs* D.I. plot (Fig. 5a). Many of the ultramafic rocks, however, do not follow the trend of the basic-intermediate types on SiO_2 *vs* D.I. plot (Fig. 5b) probably indicating a high degree of pyroxene fractionation.

The general increase in Al_2O_3 content with fractionation (*i.e.* D.I.) in ultramafic rocks (Fig. 5c) indicates that plagioclase fractionation did not take place in majority of these rocks. The decrease in Al_2O_3 with increasing fractionation in the basic-intermediate rock types, however, indicates plagioclase fractionation. As expected the anorthosites show high Al_2O_3 content. Considering anorthosites as monomineralitic cummulates, the general parallelism and/or correspondence of their overall trend with those of the gabbronorites and amphibolites on Na_2O, Al_2O_3, CaO and K_2O *vs* D.I. plots (Figs. 5a, c, d. j) indicate a genetic relationship.

The low Al_2O_3 and high CaO content in altered pyroxenite (Figs 5c, d) shows the dominant control of clinopyroxene fractionation in this rock. CaO contents are however, sufficiently low in the rest of the ultramafic rocks indica-

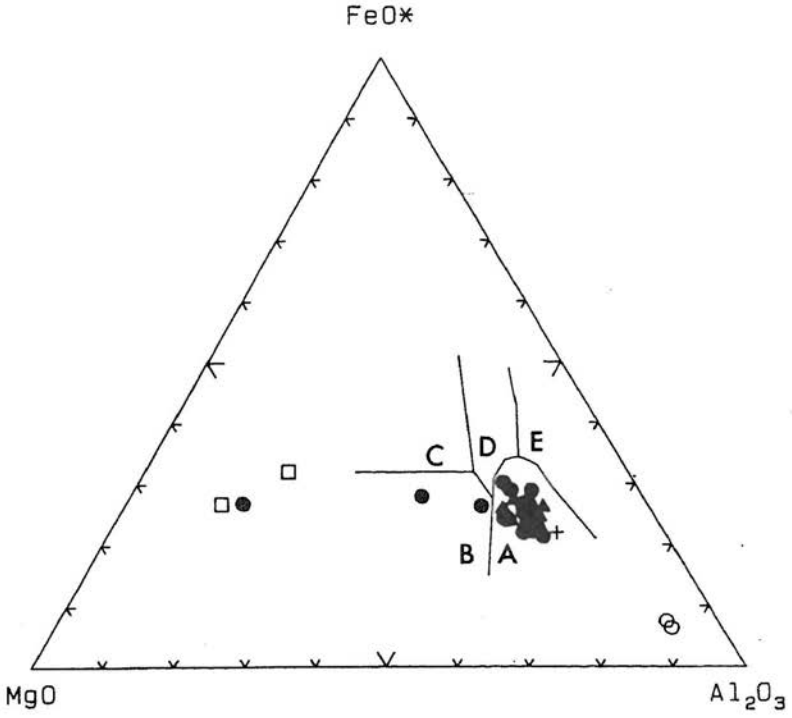

Fig. 4. Discrimination diagram showing rocks of the Chilas complex in the field for orogenic environments. A = Orogenic, B = Ocean ridge floor, C = Ocean island, D = Continental, E = Spreading centre; Pearce *et al.* (1977); Symbols as in Fig. 2.

ting that clinopyroxene fractionation in general did not take place during their production. Instead the high MgO in these rocks (*c.* 25–48 wt%, Table 1; see also Fig. 5e) points to the control of olivine and orthopyroxene fractionation on the liquidus. The scatter shown by the rocks with D.I. < 22 on FeO *vs* D.I. plots and by all the rock types in general on Fe_2O_3 and TiO_2 *vs* D.I. plots indicate the variable proportions of magnetite, titanmagnetite and ilmenite in the ultramafic rocks and of chrome spinels and sulphides in basic-intermediate types (see Asif *et al.*, 1985). All those features are interpreted as indicators of highly varied oxygen fugacities during the course of fractional crystallization and/or during metamorphism.

A considerable scatter is indicated by the P_2O_5 *vs* D.I. plot of all the rock types under investigation (Fig. 5k). The mobility of volatiles during metamorphism, especially high grade is widely advocated (Sighniolfi and Gorgini, 1978) and the scatter in P_2O_5 may be related to such phenomenon. The relatively high P_2O_5 in certain ultramafic rocks (0.1 wt.%, Table 1) is not clear; it may reflect selective mobility or analytical error.

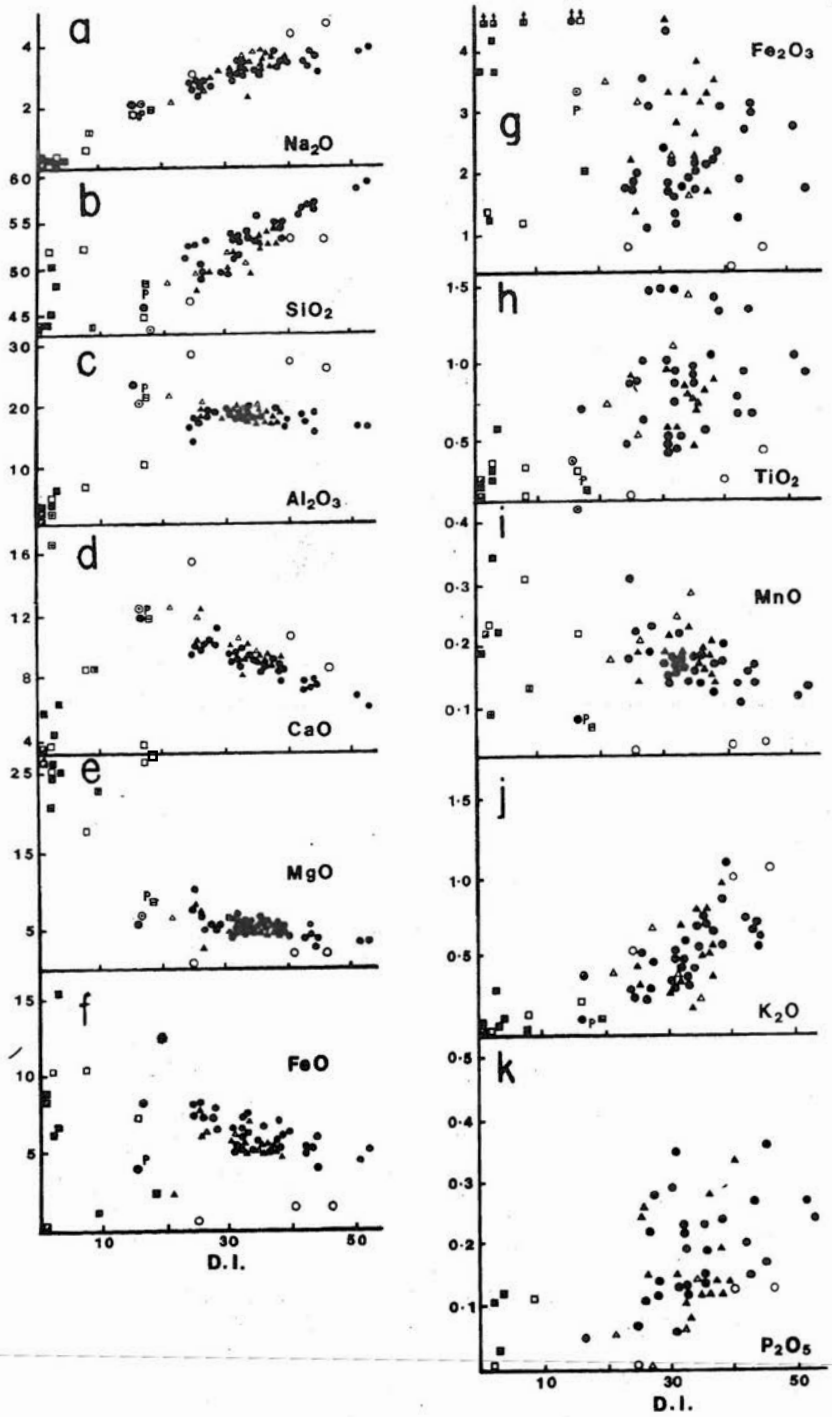

Fig. 5. Oxide *vs* Differentiation Index plots of the Chilas complex; Symbols as in Fig. 2.

The Chilas complex rocks were also plotted on oxide vs solidification index (S.I.) (plots not presented), which revealed similar petrogenetic information as obtained from oxide *vs* D.I. plots. The oxide vs S.I. plots, however, reflected more scattered patterns than shown by oxide *vs* D.I. plots; a feature indicating that the basic-intermediate rocks of the Chilas complex are close to liquid compositions.

CRYSTALLIZATION TRENDS IN CMAS MODEL

As an aid to the elucidation of petrogenesis, and in addition to more commonly used plots of chemical data, modelling has been carried out using the CMAS model (*cf.* Cox *et al.,* 1979). in conjunction with the data reduction and projection scheme of O'Hara (1976), programmed by one of us (S.H.) on the IBM–XT computer. CMAS end members are calculated from oxide wt.% (Cox *et al.,* 1979).

An olivine and/or orthopyroxene fractionation led to the formation of ultramafic rocks. This interpretation is based on the occurrence of the compositional plots of these rocks defining a trend parallel to En–Pargasite join, below the En corner, in a projection from Qtz into En–Ky–Wol plane (Fig. 6). Such plots are compatable with the early crystallization of olivine and/or orthopyroxene and the gradual replacement of these phases by clinopyroxene and/or spinel in the latter stages, on the liquidus. An orthopyroxene+plagioclase fractionation with plagioclase dominant over orthopyroxene led to the formation of basic-intermediate rock types. This is shown by the compositional plots of these rocks occurring in an elongate field which is just below pargasite-mica join and is generally parallel to the En–Feldspar join in the same projection. The greater affinities of anorthosite with the feldspar position indicate the sole control of plagioclase on the liquidus during their formation. The compositional plots of the altered pyroxenite lie close to the position of clinopyroxene. This confirms the dominant role of the clinopyroxene fractionation in this rock as suggested earlier (*cf.* Figs. 5c-d). Compositional gap between the basic-intermediate rocks and anorthosites in Figure 6 can be related to the dominance of plagioclase in the latter types. All these interpretations are supporting those suggested on the basis of oxide *vs* D.I. plots (*cf.* Fig. 5).

Corresponding features are also shown in a projection from Ky into Pl–En–Fo plane (Fig. 7a). An olivine fractionation and its subsequent replacement by orthopyroxene fractionation in the ultramafic rocks can be identified on the basis of the plot pattern of these rocks following a trend diverging from Fo apex towards En–Pl join and showing greater affinities towards En and Fo apices than towards the Pl apex. The occurrence of the plots of one of the troctolites and one of the orthopyroxenites close to the middle of the Fo–Pl join reflects a high proportion of plagioclase in these rocks compared to the rest of the ultramafic rocks. It also shows that in certain rock types plagioclase probably

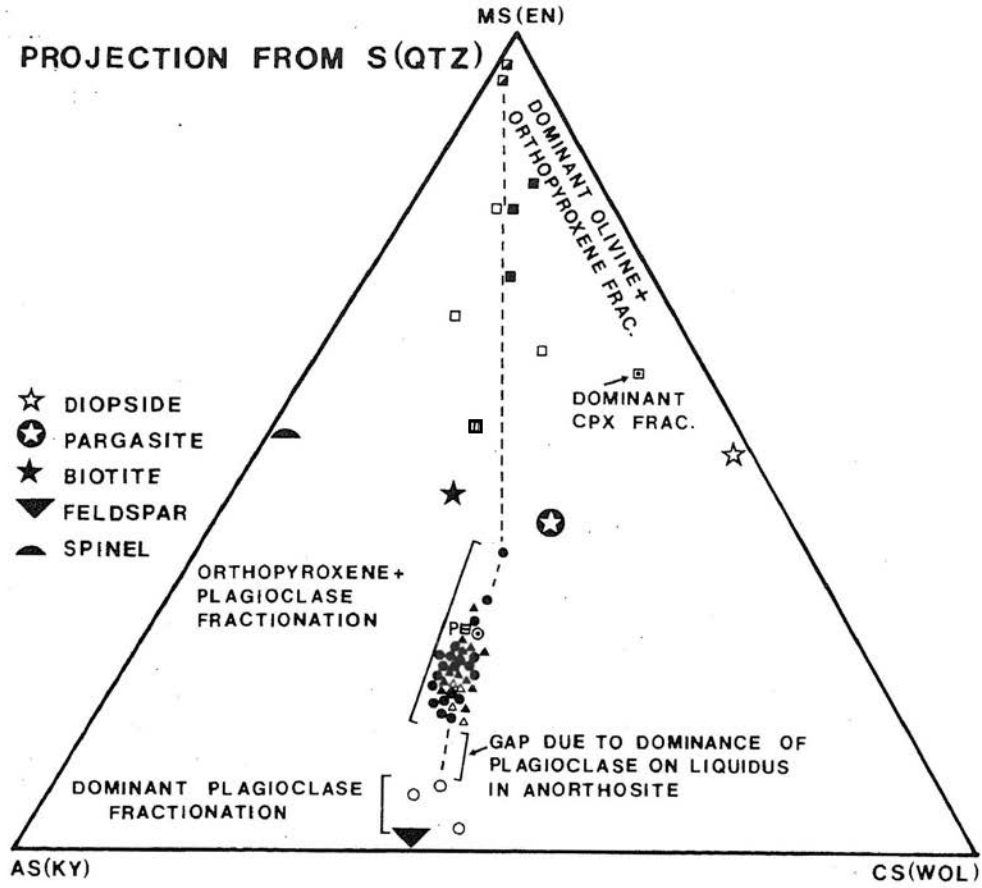

Fig. 6. CMAS plots showing fractionation trend of the Chilas complex in a projection from Qtz into En–Ky Wol plane. C–M–A–S end members were calculated using oxide wt. %; Abbreviations for theoritical end members are: Qtz = quartz, En = enstatite, Ky = kyanite, Wol = wollastonite, Pl = plagioclase, Fo = forsterite; Symbols as in Fig. 2.

appeared just after olivine on the liquidus and had a dominant role than played by pyroxene in the fractionation history of such rocks. The dominant control of the orthopyroxene and plagioclase fractionation in the early stage and the replacement of orthopyroxene by plagioclase in a later stage predicted from the plot pattern of the basic-intermediate rocks in the previous projection (Fig. 6) are also reflected. Compositional plots of some of the rock types lying on the Fo–poor side of the En–Pl join indicate greater affinities towards the En apex while compositional plots of the rest of the rocks, particularly anorthosites, show greater affinities towards the Pl apex. The altered pyroxenite plots closer to the clinopyroxene position than to the trend of the ultramafic rocks confirming the role of clinopyroxene fractionation in this particular rock. A bend in the overall trend at the intersection of the trends of the ultramafic rocks and the basic-

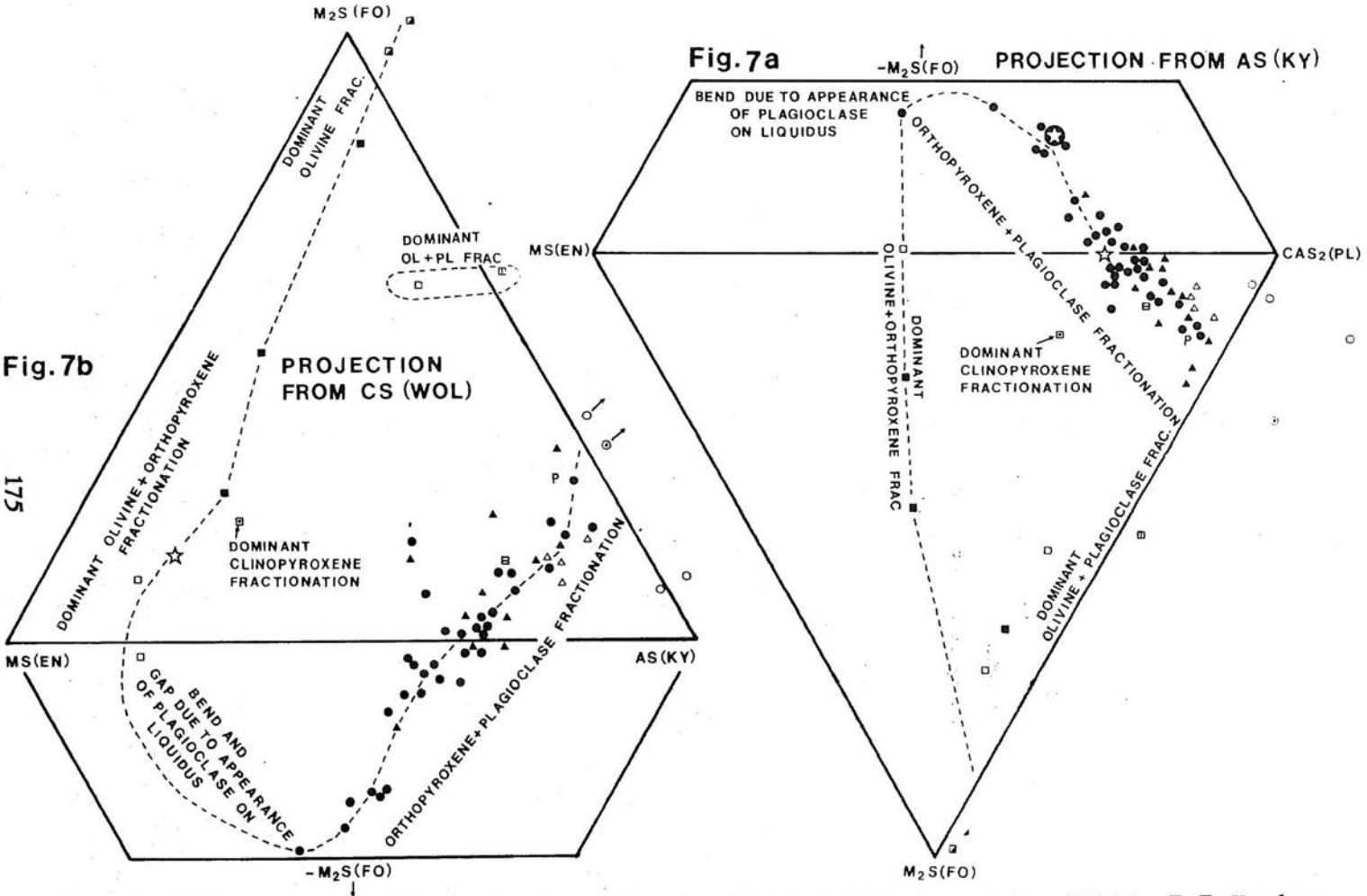

Fig. 7a–b. CMAS plots of the Chilas complex in projections from Ky into En-Fo-Pl plane and from Wol into Fo-En-Ky plane; Symbols and abbreviations are as in Figures 2 & 6.

intermediate rocks indicating the appearance of plagioclase on the liquidus in the later group can also be noticed. Majority of these features can be also confirmed from the plot pattern of the various rock types in a projection from Wol into En–Ky–Fo plane **(Fig. 7b).**

DISCUSSION

Previous workers (Asif *et al.*, 1985; Jan *et al.*, 1984) have suggested three alternative evolutionary mechanisms for the development of the Chilas complex :

a. Existence of a zoned magma chamber with a main upper portion of gabbronoritic liquid and a base of picritic composition. The crystallization of the upper part was followed by the intrusion of the picritic magma.

b. Picritic magma intruded from deeper levels at the base of a crystallizing magma chamber of gabbronoritic composition.

c. All the rocks types of the Chilas complex have crystallized from one and the some magma and the ultramafic rocks represent remobilised early cummulates.

The continuous variation and general correspondence in major element chemistry of the various basic and intermediate types, reflected in oxide *vs* D.I. and CMAS plots, indicate an igneous parentage, the control of crystallization differentiation and a genetic relationship among the various rock types of the Chilas complex. The same features are also indicated by the general parallelism or correspondence of the chemical trend of the cummulative rocks (ultramafic rocks and anorthosites) with those of the gabbronorites and amphibolites on many of the variation diagrams and thus favour the third possibility mentioned above (*cf.* Fig. 5a, c, d, j). Bends and gaps in the variation trends are considered to be related to the appearance and disappearance of various phases on the liquidus, however, the gaps may simply be due to the lack of representative samples.

The affinity diagrams (Fig. 2–4) show that the various rock types of the Chilas complex have crystallized from a basic magma of calcalkaline character. The extensive volume ot the gabbronorites may, however, be related to crystallization of this magma in more than one magma chambers.

The development of the ultramafic rocks has been considered as a result of dominant olivine fractionation subsequently accompanied and replaced by orthopyroxene fractionation. A genetic relationship between these rocks and gabbronorite has been already mentioned above. No olivine relics have been, however, noticed in gabbronorites. Considering crystallization in a Fo–En–SiO_2 system (Anderson, 1915), this feature can be related to the accumulation of most of the olivine, resulting in the production of what is now dunite and peridotite

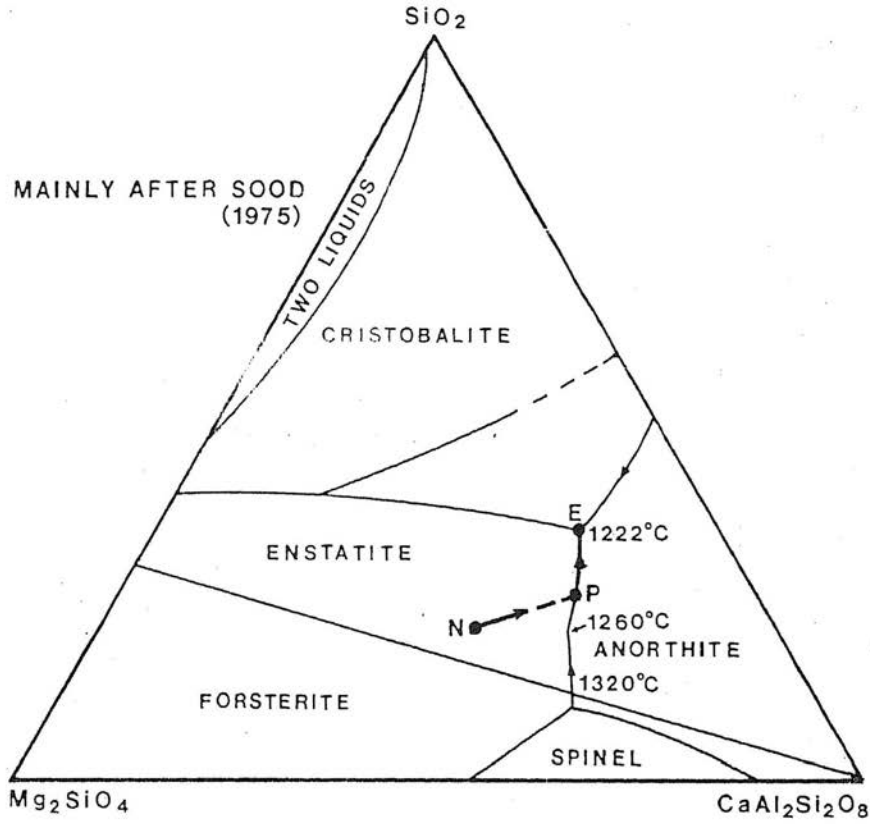

Fig. 8. Hypothetical crystallization path (N–P–E) of the Chilas complex rocks in system Mg_2SiO_4–$CaAl_2Si_2O_8$–SiO_2.

at the base(s) of hypothetical magma chamber(s) and to the complete resorption of the remaining olivine crystals in the stability field of orthopyroxene. The complete resorption of olivine will occur only if the original magma composition lies in the stability field of protoenstatite, more or less close to composition 'N' in a Mg_2SiO_4–$CaAl_2Si_2O_8$–SiO_2 system (Fig. 8). The calcalkaline characters suggested for the parent liquid of the rocks of the Chilas complex may correspond to such a hypothetical magma composition. Ignoring the crystallization of the minor proportion of spinel in the early stages of fractionation history, such a composition is expected to crystallize olivine but will react to form enstatite from all the existing olivine under equilibrium conditions. With crystallization of orthopyroxene the changing residual liquid composition will follow a path N–P towards the En–An boundary and at P both enstatite and plagioclase will crystallize together (see Sood 1980, p. 24). Such a crystallization model is consistent with that postulated for the gabbronorites on the basis of CMAS plots as with

the presence of very minor proportions of normative olivine in a few gabbronorites. These may have disappeared during metamorphism (Jan, 1977a). As mentioned earlier the occurrence of ultramafic rocks at the present level of erosion and seemingly intrusive into gabbronorites can be attributed to the emplacement of the former types as plastically remobilised bodies into the later type *(cf.* Jan, 1980, 1983).

Orthopyroxenite and anorthosite occur in layers, generally interbedded with main gabbronorite. Inspite the fact that rocks of the Chilas complex have undergone a considerable polyphase deformation, the layers are considered to be of igneous origin. Extreme type pyroxenite and anorthosite are generally scarce, and in contrast to the known layered complexes *(i.e.* Bushvald and Stillwater), there is no evidence of a specific horizon to indicate the confinement of orthopyroxenite or anorthosite to the base of the complex. These features and the CMAS plots together indicate that orthopyroxenite, anorthosite and gabbronorite probably developed during the alternating episodes of the dominance of orthopyroxene or plagioclase or orthopyroxene+plagioclase, respectively, on the liquidus along P–E in the Mg_2SiO_4– $CaAl_2Si_2O_8$–SiO_2 system (Fig. 8). The decrease on the liquidus, in the proportion of plagioclase during the formation of pyroxenite and of orthopyroxene during the formation of anorthosite can be explained on the basis of compositional variations, particularly Al_2O_3 content of the liquid. Breman (1983) studying the behaviour of crystallization in CaO–MgO–Al_2O_3–SiO_2 system at 1 atm. pressure found that basaltic liquids containing Al_2O_3 15 wt. % did not crystallize plagioclase. Instead clinopyroxene and orthopyroxene were the dominant phases on the liquidus. Anorthite appeared on the liquidus at the expense of diopside when the Al_2O_3 content of the liquid reached upto 15 wt.%. At 20 wt% Al_2O_3 the enstatite stability field started shrinking and at 25 wt.% Al_2O_3 enstatite was also no more a stable phase. These evidences, and the presence of the plagioclase fractionation shown by the chemistry of the majority of the rocks from the Chilas complex, indicate that Al_2O_3 content of the liquid from which orthopyroxenite, anorthosite and the gabbronoritic members crystallized, was more or less in the range of *c.* 15–20 wt. %. This interpretation is consistent with the Al_2O_3 contents of most of the gabbronorite compositions (see Table 1). It also explains the dominance of orthopyroxene over clinopyroxene in the suite. In addition the content of Al_2O_3 must have been varying with crystallization, resulting in a variable proportions of orthopyroxene, clinopyroxene and plagioclase and thus, giving rise to interbedded gabbronorite (pyroxene granulite) pyroxenites and anorthosite.

Majority of the main gabbronorite compositions indicate normative quartz while modal quartz is present in these rocks and its proportion increases in the intermediate members. Inclusions of quartz have been also noticed in other minerals *(cf.* Jan, 1979). These features suggest that due to the crystallization of orthopyroxene and plagioclase in gabbronorite, orthopyroxenite and anorthosite,

the residual liquid successively became richer in SiO_2, and quartz appeared on the liquidus at the later stages of the noritic crystallization. This interpretation is consistent with the crystallization of anorthite and enstatite along the eutectic path P–E and association of tridymite with these phases at cotectic E, in a Mg_2SiO_4–$CaAl_2Si_2O_8$–SiO_2 system (Fig. 8). The development of a silica mineral at the final stage of crystallization in noritic magma is also consistent with the consideration of the composition of the original liquid as being closer to 'N' in the Mg_2SiO_4–$CaAl_2Si_2O_8$–SiO_2 system. Crystallization along path P–E in Figure 8, from an original magma composition more basic than 'N' may terminate before the residual magma composition reaches E and thus may not crystallize a silica mineral as the final phase on the liquidus *(see* Sood 1981 p. 25–26).

Compositional plots of the altered pyroxenite in the various projections of the CMAS model indicate the dominant control of clinopyroxene fractionation. Modal clinopyroxene has also been noticed in gabbronorite and some other rocks. These features indicate that clinopyroxene has also played some role in the evolution of rocks of the Chilas complex. Considering the crystallization of such clinopyroxene with orthopyroxene and plagioclase, a temperature of about 1200°C and pressure of < 10 kb are suggested for the development of this assemblage in the Chilas complex. This assumption is based on experimental data in a projection from CMS_2 into MgO–$CaAl_2O_4$–SiO_2 plane of the CMAS system (see Basaltic volcanism study project, 1981, p. 598, Fig. 3.6.1A), and the supposition that igneous crystallization has followed a path N–P–E in the Mg_2SiO_4–$CaAl_2Si_2O_8$–SiO_2 system (Fig. 8). This would in turn show that the presumed magma chamber(s) in which the crystallization occurred, existed at a depth of < 35 km. According to Jan (1977a) the pyroxene granulite facies metamorphism occurred at a depth of about 25 km (pressure of 5.5–7 kb) and the nearby garnet granulites of the Jijal ultramafic complex indicate further recrystallization of the pyroxene granulite at a depth of > 40 km. All these features indicate that either the gabbronorite, anorthosite and ultramafic rocks of the Chilas complex originated in magma chamber(s) at a depth of 25 km and were later on recrystallized under the granulite facies conditions due to subduction, folding or increase in thickness of the overlying volcanic piles or the whole igneous crystallization occurred under the pyroxene granulite facies condition, *i.e.* at a depth of about 25 km. *(cf.* Jan, 1980).

The amphibolite bodies intimately associated with gabbronorite (pyroxene granulite) *(cf.* section 1) have been considered as the retrograde products of the pyroxene granulites, mainly due to the influx of water during obduction (Jan 1980). The genetic relationship shown by the major element chemistry of the two types supports such a view.

Jan (1977) has put forward several views about the source material for the parent magma of the Chilas complex. With the present limited data avail-

able it is difficult to support any view point. However, the calcalkaline affinities and similarities of the suite to major plutonic rocks of island arcs suggest that its origin was in some way related to subduction of an oceonic lithosphere during the formation of the Kohistan island arc. This view is further corroborated by the similarity of mineral phases in the Chilas complex and island arcs plutonic rocks (Jan, unpublished data).

CONCLUSIONS

1. The gabbronorites, amphibolites, peridotites, pyroxenites, troctolites and olivine gabbros, and anorthosites of the Chilas complex represent a cognate magmatic suite of rocks produced as a result of crystallization differentiation from a parent magma of calcalkaline characters, originated in arc-related orogenic environments.

2. Olivine was the earliest mineral on the liquidus followed and subsequently replaced by orthopyroxene.

3. Accumulation of olivine to the base(s) of magma chamber(s) was probably responsible for the development of olivine-rich cummulate rocks.

4. Orthopyroxene was accompanied by plagioclase on the liquidus and orthopyroxenite, gabbronorite and anorthosite developed as a result of dominance of orthopyroxene, orthopyrovene+plagioclase and plagioclase, respectively, on the liquidus at the various stages of crystallization differentiation. The dominance of these particular phases on the liquidus, at a particular time, was probably controlled by the changing magmatic composition (especially Al_2O_3 content) and/or pressure due to crystallization. It is, however, likely that the compositional variations observed were a product of several combined processes including crystallization differentiation, accumulation, crystal sorting and subsequent compaction of the cummulate piles.

5. Plagioclase associated with and/or replaced olivine locally on the liquidus which led to the development of troctolite, olivine gabbro and feldspathic peridotite.

6. Quartz crystallized as one of the final products of crystallization differentiation from the residual liquid.

7. The major part of crystallization probably occurred at a temperature of about 1200°C and at a depth of < 25 km.

8. Recrystallization of the rocks under the pyroxene granulite facies environment was probably due to subduction, folding or increase in thickness of the volcanic piles to a depth of 20–25 km.

9. The genetic relationship of the gabbronorites and amphibolites revealed by the chemistry of these rocks confirms that the latter type is the retrogressive metamorphic product of the former.

10. Ultramafic rocks probably represent genetically related early cummulates remobilized into gabbronorites.

Acknowledgement : Much of the analytical work for this study was carried out in King's College London, as part of the Ph.D. research project of one of the authors (M.Q.J.) and was kindly supported by the British Council. Professor R.A. Howie and J.N. Walsh are thanked for their valuable suggestions and Munir Humayun for critically reading the manuscript.

REFERENCES

Anderson, O., 1915. The system anorthite-forsterite-silica. Am. J. Sci. 39, 407—454.

Asif, M., Habib, M. & Jan M.Q., 1985. Ultramafic and mafic rocks of Thurly Gah and their relationship to the Chilas complex, N. Pakistan. Geol. Bull. Univ. Peshawar, 18, 83—102.

Bard, J.P., Maluski, H., Matte, Ph. & Proust, F., 1980. The Kohistan sequence: crust and mantle of an obducted island arc. Geol. Bull. Univ. Peshawar (Spec. Issue) 13, 87—94.

Basaltic volcanism study project, 1981. Basaltic volcanism on terrestrial planets. Pergamon Press, Inc. New York, 1285 pp.

Berman R.G., 1983. A thermodynamic model for multicomponent melts, with application to system CaO–MgO–Al_2O_3–SiO_2. Ph.D. thesis, Univ. British Columbia, (unpubl.).

Chaudhry, M.N. & Chaudhry, A.G., 1974. Geology of Khagram area, Dir District. Geol. Bull. Punjab Univ. 11, 21—43.

Chaudhry, M.N., Kausar, A.B. & Lodhi, S.A.K., 1974. Geology of Timurgara-Lal Qila area, Dir District, N.W.F.P. Geol. Bull. Punjab Univ. 11, 53—73.

Cox, K.G., Bell, J.D. & Pankhurst, R.J., 1979. The interpretation of igneous rocks, George Allen & Unwin, London.

Jan, M.Q., 1977a. The mineralogy, geochemistry and petrology of Swat Kohistan, NW Pakistan. Ph.D. thesis, Univ. London (unpubl.).

Jan, M.Q., 1977b. The Kohistan basic complex: a summary based on recent petrological research. Geol. Bull. Univ. Peshawar, 9—10,36—42.

Jan, M.Q., 1979. Petrography of the amphibolities of Swat and Kohistan. In: Geology of Kohistan (R.A.K. Tahirkheli and M.Q. Jan eds.), Geol. Bull. Univ. Peshawar (Spec. Issue) 11, 51—64.

Jan, M.Q., 1980. Petrography of the obducted mafic anl ultramafic metamorphites from the southern part of the Kohistan island arc sequence. Geol. Bull. Univ. Peshawar (Spec. Issue) 13, 95—107.

Jan, M.Q. & Howie, R.A., 1980. Ortho- and clinopyroxenes from the pyroxene granulite of Swat Kohistan, northern Pakistan. Mineral. Mag. 47, 715—726.

Jan, M.Q., Khattak, M.U.K., Parvez, M.K. & Windley, B.F., 1984. The Chilas stratiform complex: field and mineralogical aspects. Geol. Bull. Univ. Peshawar, 17, 153—169.

Jan, M.Q. & Kempe, D.R.C., 1973. The petrology of the basic and intermediate rocks of upper Swat, Pakistan, Geol. Mag. 110, 285—300.

O'Hara, M.J., 1976. Data reduction and projection scheme for complex compositions. In: Progress in experimental petrology. N.E.R.C. Publ. Ser. D(6). 103—126.

Schwarzer, R.R. & Rogers, J.J.W., 1974. A worldwide comparison of alkali-olivine basalts and their differentiation trends. Earth Planet. Sci. Lett. 23, 286—296.

Shams, F.A., 1975. The petrology of the Thak valley igneous complex. Gilgit agency, Northern Pakistan. Accad. Zaz. Linci, Ser. 8, v. 59, 453—464.

Sighinolfi, G.P. & Gorgoni, C., 1978. Chemical evolution of high grade metamorphic rocks — anatexis and remotion of material from granulite terrains. Chem. Geol. 22, 157—176.

Sood, M.K., 1980. Modern igneous petrology. Wiley & Sons, New York.